

Flux-Canceling Electrodynamical Maglev Suspension: Part I Test Fixture Design and Modeling

Marc T. Thompson, *Member, IEEE*, Richard D. Thornton, *Life Fellow, IEEE*, and Anthony Kondoleon

Abstract—The design and analysis of a scale-model suspension test facility for magnetic levitation (maglev) is discussed. We describe techniques for the design, construction, and testing of a prototype electrodynamic suspension (EDS) levitation system. The viability of future high-temperature superconducting magnet designs for maglev has been investigated with regard to their application to active secondary suspensions. In order to test the viability of a new “flux-canceling” EDS suspension, a 1/5-scale suspension magnet and guideway was constructed. The suspension was tested by using a high-speed rotating test wheel facility with linear peripheral speed of up to 84 m/s (300 km/h). A set of approximate design tools and scaling laws has been developed in order to evaluate forces and critical velocities in the suspension.

Index Terms—Control systems, high-temperature superconductors, inductance, levitation, magnetic analysis, magnetic forces, magnetic levitation, maglev, modeling, superconducting coils, superconducting magnets.

I. INTRODUCTION

ELECTRODYNAMIC magnetic suspension, called EDS magnetic levitation (maglev) and referred to as repulsive maglev because it relies on repulsive magnetic forces, has the capability of allowing high speed transportation with a relatively large gap between the vehicle and guideway. In 1966 Danby and Powell [1]–[3] proposed an EDS system for high-speed transportation using superconducting magnets with a “null flux” suspension. Other designs were later proposed using continuous sheet guideways ([4]–[9], among others). Subsequent researchers in the United States, Japan, Germany, United Kingdom, and Canada have developed further innovations (such as the use of a ladder-type guideway for increased lift efficiency), but there are still a number of technical problems that need resolution.

The first recorded proposal for an attractive magnetic suspension was by Graeminger [10] in 1911 with a U-shaped electromagnet carried on a vehicle suspended below an iron rail with feedback maintained by sensing a mechanical or pressure sensor. To date the only commercial maglev imple-

mentations have used the electromagnetic suspension (EMS) in which electromagnets support a vehicle with attractive forces to steel guideways. While EMS may be a preferred option for lower speed designs, it has the fundamental disadvantage of requiring a small gap between the vehicle and guideway, typically less than a centimeter, and requires active control to maintain the gap. The promise of EDS is that this gap can be increased by a factor of five or more, and therefore guideway tolerances are relaxed and cost reduced.

Another purported advantage of EDS is that it can be inherently stable and not dependent on feedback control to maintain a constant gap. Unfortunately, this advantage is not as real as it appears because all EDS designs are highly underdamped and, in certain cases, even unstable [11]–[18]. Other disadvantages of EDS are higher power requirements for suspension, higher external magnetic fields, and the need for a separate low speed suspension. Nevertheless, prototype EDS trains have been successfully operated at speeds up to 550 km/h in Japan.

The foremost problem for all high speed ground transportation systems is the high cost of guideway construction, but this key issue is not unique to maglev. Many researchers are now convinced that if maglev technology were fully developed it would be less expensive than a high speed train if all installation and operating costs are compared. This is particularly true if the maglev system can provide shorter travel times which in turn attracts more users so that the capital cost per user is reduced. The reason for the EMS preference has been its apparently lower cost because it uses a relatively simpler technology with fewer unknowns. German maglev developers have shown that EMS can operate successfully at speeds over 400 km/h, so the problem is to improve EDS to the point that, for high speed travel, it has substantial advantages other than that of a larger gap.

We believe that a successful EDS design must face squarely the following problems.

- The cost of manufacturing and installing suspension and propulsion components on the guideway must be reduced to an absolute minimum.
- The suspension system must have a power loss that is comparable to that for EMS.
- All EDS suspension designs are highly underdamped and it is imperative to find practical means to damp oscillations and provide high ride quality.
- External magnetic fields associated with onboard superconducting magnets must be reduced, particularly in the passenger compartments.

Manuscript received June 3, 1998; revised January 11, 1999.

M. T. Thompson was with the Laboratory for Electromagnetic and Electronic Systems, Massachusetts Institute of Technology, Cambridge, MA 02139 USA. He is now at 25 Commonwealth Road, Watertown, MA, 02472 (e-mail: marctt@aol.com) and with Worcester Polytechnic Institute, Worcester, MA 01609 USA.

R. D. Thornton was with the Department of Electrical Engineering and Computer Science, Massachusetts Institute of Technology, Cambridge, MA 02139 USA. He is now with Magnemotion, Inc., Sudbury, MA 02776 USA (e-mail: mmi-rdt@magnemotion.com).

A. Kondoleon is with the Charles Stark Draper Laboratory, Cambridge, MA 02139 USA.

Publisher Item Identifier S 0018-9464(99)02790-9.

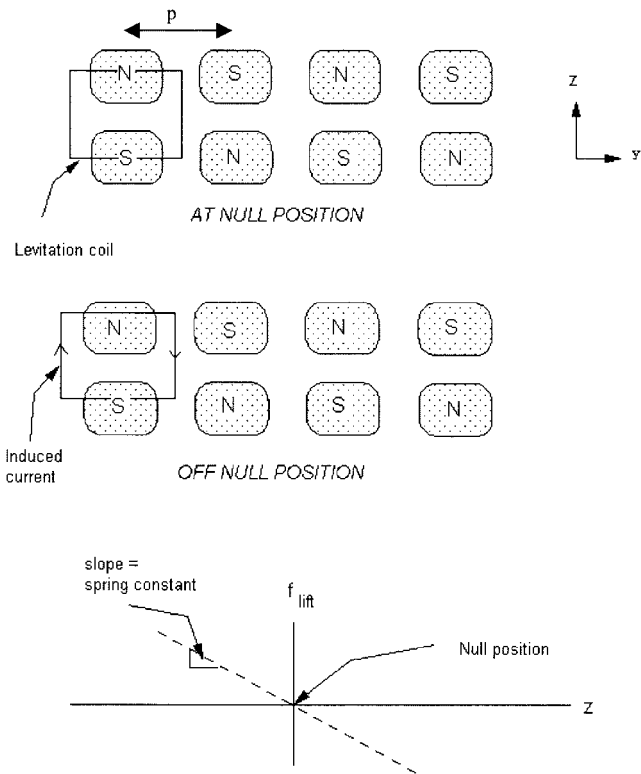


Fig. 1. Flux-canceling maglev topology. Top: train at null position, no induced currents. Middle: train above null position. Currents are induced, creating a restoring force. Bottom: magnetic spring constant.

- It is highly desirable to eliminate the need for a separate low speed suspension system because this adds to the cost, weight, and complexity of both the vehicle and guideway.
- Any superconducting vehicle magnets must be able to operate reliably in a hostile transportation environment.

This and a companion paper in these TRANSACTIONS report the latest results of MIT research to develop an improved EDS design that addresses all of these issues.

II. MAGLEV TEST FIXTURE DESIGN

This section describes the design and modeling of the multiple-loop guideway and development of circuit models to predict behavior of a novel maglev system based on a high-temperature superconducting coils. This so-called “flux-canceling” EDS maglev suspension achieves high efficiency for suspension and guidance in addition to rapid attenuation of magnetic flux with distance [19], [20] by utilizing an iron core and superconducting octapoles. In order to test these concepts, a 1/5-scale suspension magnet using copper coils and guideway embedded in a high-speed rotating test wheel was constructed. Details of the test fixture design and analysis are given in several papers and a Ph.D. dissertation by one of the authors [21]–[24].

A. Flux-Canceling Geometry

The guideway is composed of multiple conductive copper coils arranged vertically, and the train magnets are arranged in a dual-row north-south-north-south (N-S-N-S) arrangement (Fig. 1). When the train is in the vertical null position at

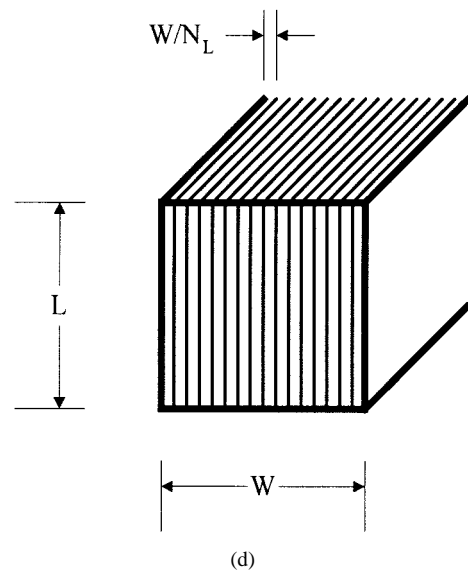
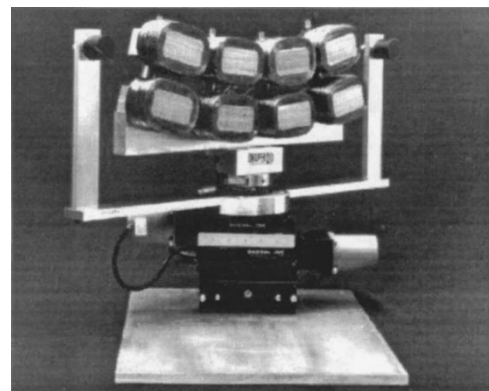
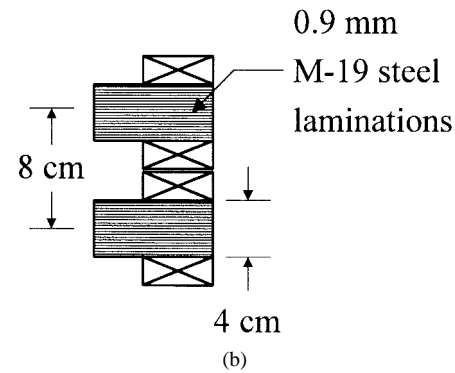
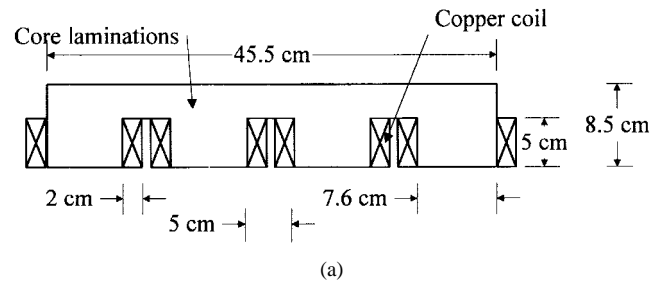


Fig. 2. Detail of magnet design. (a) Side view of linearized iron-core magnet with copper coils. (b) Rear view of dual-row magnet. (c) Iron-core suspension magnet, mounted to multi-axis force sensor, showing capacitive position sensors. (d) Core laminations.

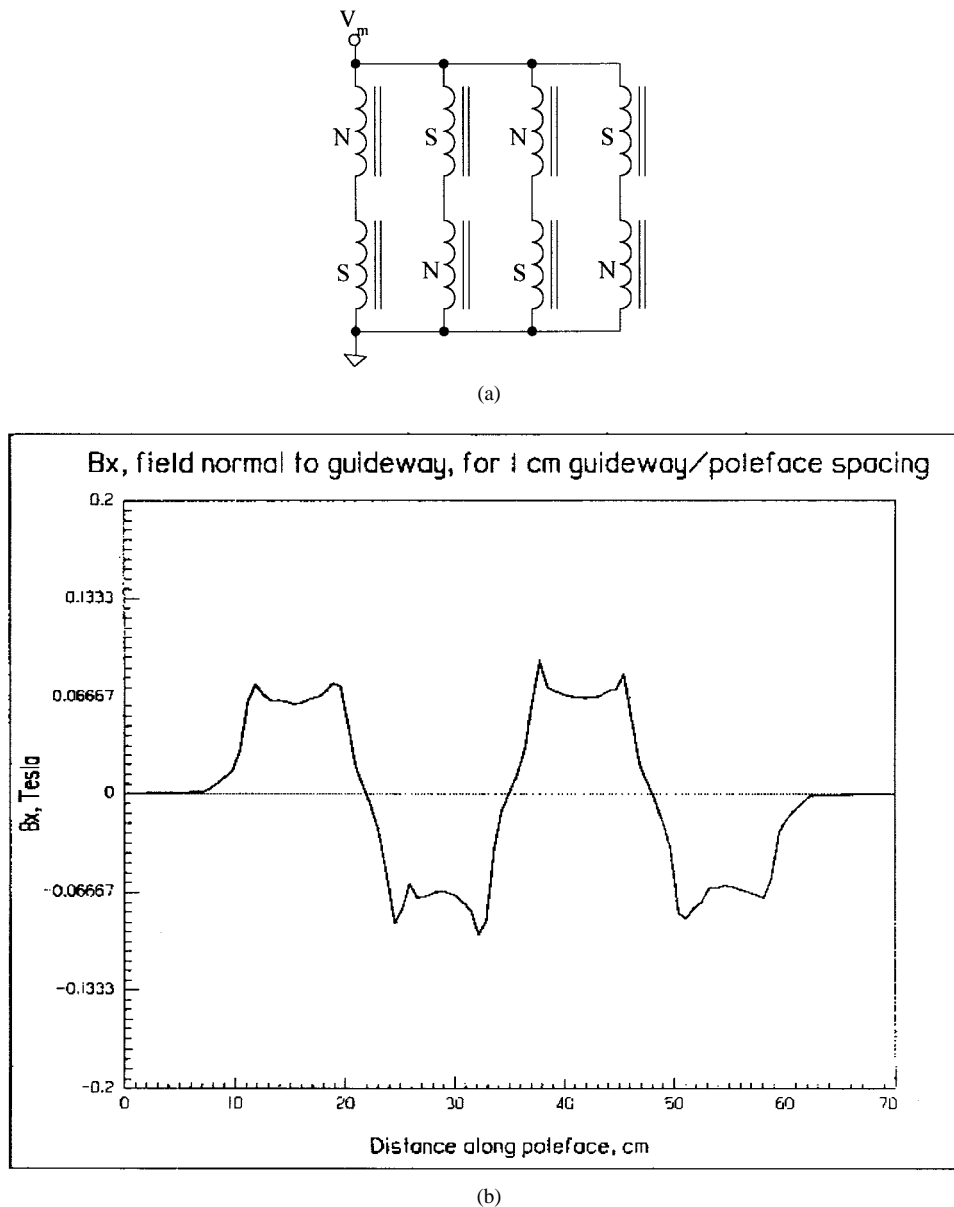


Fig. 3. Flux-canceling maglev electrical wiring. (a) Magnet wiring for flux-canceling maglev. (b) Results of finite element analysis, $NI = 2200$ Ampere-turns per coil.

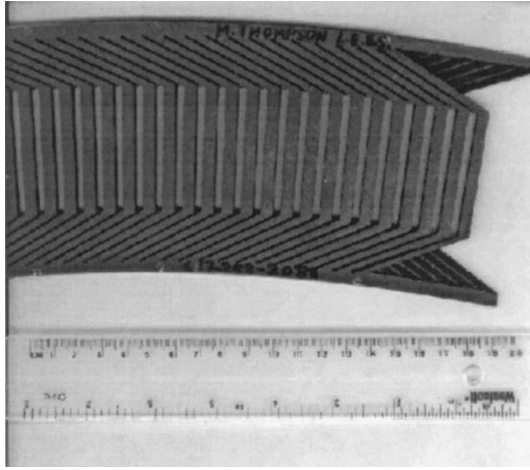
$z = z_0$ and traveling in the $+y$ direction, there is no net flux through the levitating coils and no net current induced around the loop. However, if the train's vertical position deviates from equilibrium, the net changing flux through the loop induces currents in the loop. This creates a restoring force, with the magnetic suspension acting as a linear spring with spring constant k_z . The suspension has a resulting resonant frequency $\sqrt{k_z/M}$ where k_z is the magnetic spring constant and M is the total suspended mass. There is no inherent damping mechanism intrinsic to EDS suspensions other than aerodynamic drag.

B. Suspension Magnet Design

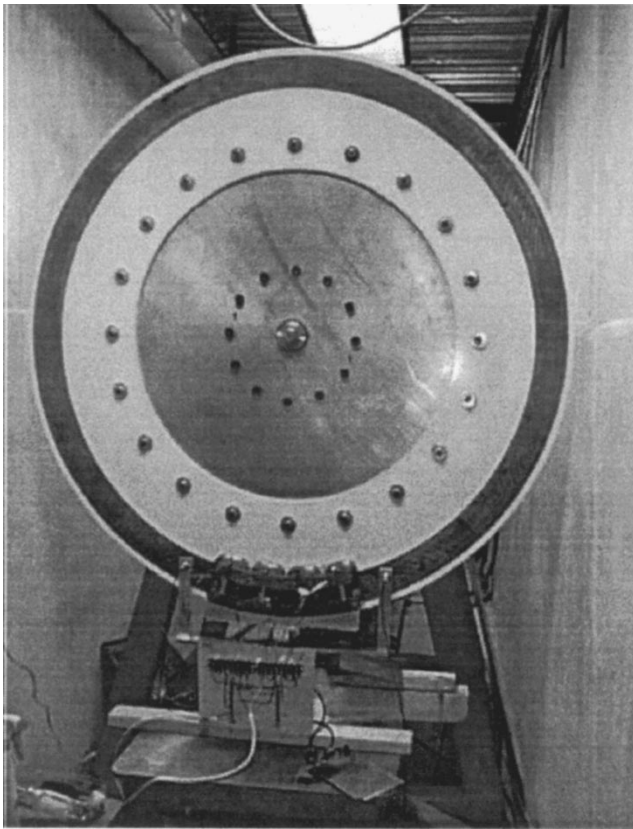
The suspension magnet in the test facility has a pole pitch $p = 0.126$ m. A linearized view of the magnet with copper

coils is shown Fig. 2. The magnet core is constructed with laser-cut laminations of 0.9 mm thick M19 transformer steel. Eight copper coils were wound with 18 gauge copper magnet wire on an arbor with the same geometry as the magnet polefaces. The final copper coil design had 550 turns in a winding window of 5 cm \times 2 cm. The design limit of the copper coils is 8 amps in still air (with current density $J \approx 1000$ A/cm²) and 20 amps when operating in the liquid nitrogen bath ($J \approx 2500$ A/cm²). The measured resistance of each coil is 3.4 Ω at 300 K and 0.442 Ω when cooled to 77 K, corresponding to a maximum copper power dissipation per coil of ~ 200 watts.

The magnet is mounted to a multi-axis force sensor which allows real-time measurement of forces and moments. The core laminations were sized by considering the power dissipation per unit length in a section of the core made up of N_L



(a)



(b)

Fig. 4. Steps in maglev test wheel construction. (a) Prototype guideway section showing two copper layers bolted and brazed along the edge. (b) Completed test wheel mounted and ready for high-speed operation.

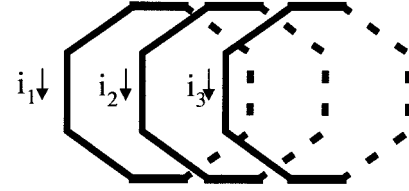
laminations [Fig. 2(d)] calculated to be [25]

$$P \approx \frac{\sigma L W^3 \left(\frac{dB}{dt} \right)^2}{16 N_L^2}. \quad (1)$$

The power loss may be made arbitrarily small by reducing the thickness of the lamination. With a core design with $\sigma \approx 10^6$ $(\Omega\text{m})^{-1}$, $N_L = 40$, and expected AC fields of $\Delta B < 0.5$ Tesla at frequencies $f < 10$ Hz, the power loss in the core is calculated to be less than a watt.



(a)



(b)



(c)

Fig. 5. Guideway geometry and modeling. (a) Linearized geometry of guideway coils. (b) Broken up into individual coils (exploded view). (c) Rim.

The magnets were designed so that the top row of coils are operated in a N-S-N-S arrangement [Fig. 3(a)], while the bottom row is offset by one half cycle. The resultant magnet behaves as a magnetic octapole. A significant advantage of the magnetic octapole is the rapid far-field falloff in the field, which reduces the shielding required to maintain a low magnetic field in the passenger cabin [20].

Finite element analyses were run on the nonlinear iron core design [Fig. 3(b)]. The flux density normal to the guideway (B_x) was calculated at a distance $x = 1$ cm from the poleface of the magnet, which is the nominal setpoint for guideway-to-poleface setting. This analysis was checked against measurements taken with a Gaussmeter on the magnet operating with copper coils. The measured value at the center of the poleface was $B_x = 0.069$ Tesla, which matches the calculated value to within a few percent.

C. Guideway Coil and Test Wheel Mechanical Design

A novel multiple-loop guideway was designed which allows simple and inexpensive manufacturing. The guideway conductor pattern was constructed from 0.093 in thick sheets of 1/2 hard #110 copper. The repeating conductor pattern was cut with a high-pressure numerically-controlled water jet cutter, from 35 in \times 12 in sections of copper [Fig. 4(a)] in a 60° arc. In a full-scale system the guideway would probably be constructed from sheets of aluminum, but copper was easier to use for the initial prototype.

It is important to note the difference between this structure and a guideway made of unconnected, staggered single loops. The rim connection of adjacent loops are connected electrically through the top and bottom rims. Therefore, induced currents

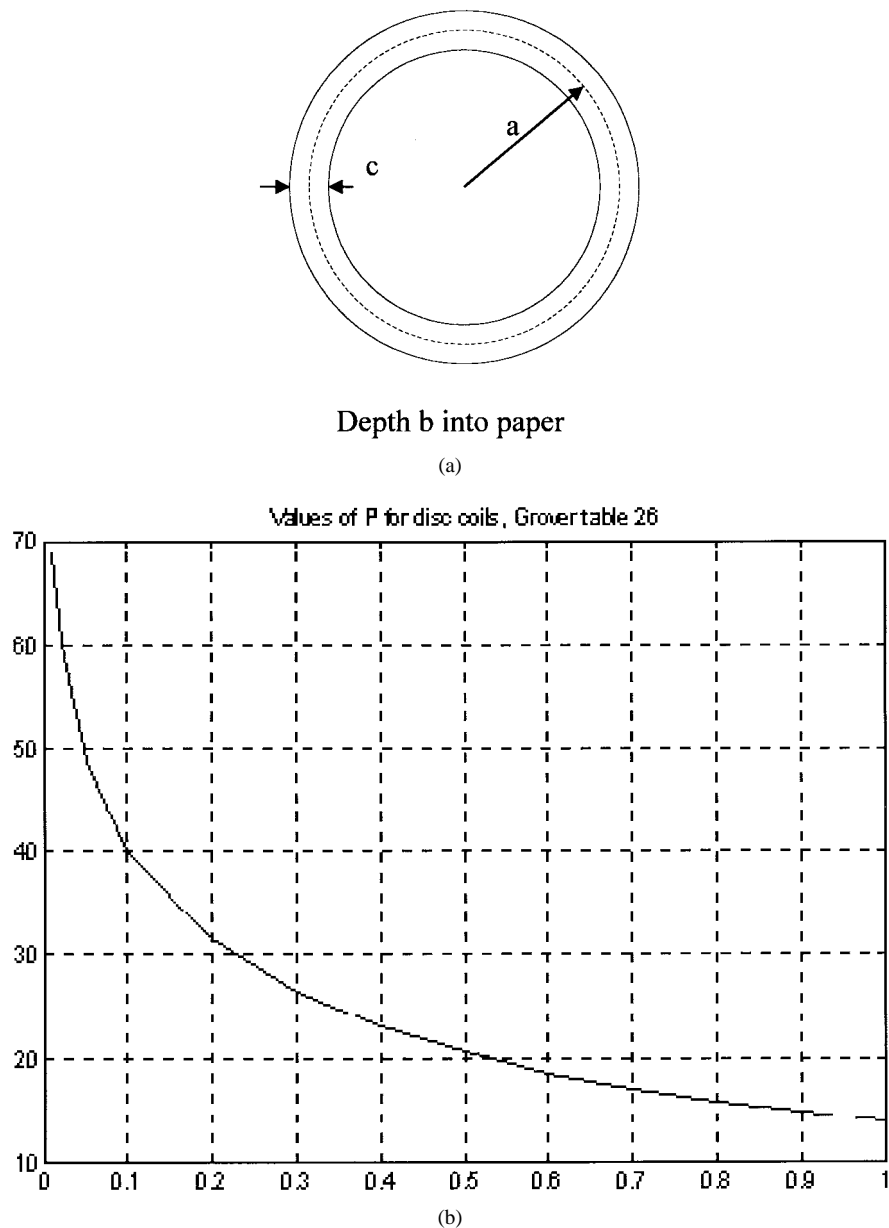


Fig. 6. Inductance modeling of circular coil with rectangular cross section. (a) Top view of disk coil. (b) Function P , for disk coils.

are not confined to single loops, and can take multiple paths. This distributed guideway has a lower maglev "drag peak" velocity than unconnected multiple loops.

After the individual guideway sections were cut, the inner face of the copper conductor pattern was painted with an electrically-insulating paint. The conductor pattern was brazed on the inner and outer radii to ensure good electrical joints and high mechanical strength. After brazing, the eccentricity of the copper ring was measured and found to be true within 1/16 of an inch. A precision mold was constructed, and a composite disk of fiberglass cloth and epoxy 5/8 in thick was constructed over the copper conductors with the conductors near one surface of the disk.

The finished test wheel was mounted to an aluminum hub with a 3 in diameter shaft, shown mounted and ready for operation in Fig. 4(b). A 10-HP motor and computer control allows adjustment of the wheel speed from 0–1000 RPM, with

a linear peripheral test speed of 0–84 m/s (0–300 km/h). A transparent coating of epoxy was used on the front face of the wheel so that the copper conductor pattern is visible.

III. MODELING OF FLUX-CANCELING SUSPENSION

Simple models were developed to demonstrate the effects of mutual coupling between guideway loops on the lift and drag forces and drag peak velocity. The goal of our modeling process was to provide useful models without relying on significant finite-element analyses and to generate approximate answers and scaling laws useful for engineering design.

A. Loop-Loop Interactions

The linearized infinite ladder guideway [Fig. 5(a)] may be broken up into individual loops [Fig. 5(b)] and a rim [Fig. 5(c)]. A very simplified view of the infinite guideway

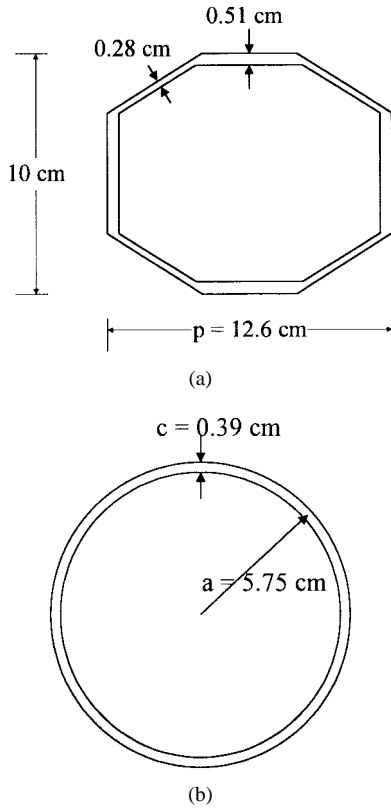


Fig. 7. Coil model, showing primitive coil section and disk coil used for approximate modeling. (a) Actual linearized geometry of one pole-pitch wide primitive guideway loop. (b) Approximate model, using disk coil enclosing same perimeter.

(given for illustrative purposes only) is a three-coil model [Fig. 5(b)]. The relationship between loop currents and induced loop voltage in the sinusoidal steady state is

$$j\omega L \begin{bmatrix} 1 & k_{12} & k_{13} \\ k_{12} & 1 & k_{12} \\ k_{13} & k_{12} & 1 \end{bmatrix} \begin{Bmatrix} i_1 \\ i_2 \\ i_3 \end{Bmatrix} + R \begin{bmatrix} 1 & r_{12} & r_{13} \\ r_{12} & 1 & r_{12} \\ r_{13} & r_{12} & 1 \end{bmatrix} \begin{Bmatrix} i_1 \\ i_2 \\ i_3 \end{Bmatrix} = \begin{Bmatrix} v_1 \\ v_2 \\ v_3 \end{Bmatrix} \quad (2)$$

where ω is radian frequency of the excitation caused by the moving superconductor coils. The self inductance of each loop is L and the loop-loop mutual inductance $M_{ij} = k_{ij}L$ where k_{ij} is the loop coupling coefficient which is less than one. The effects of a shared rim on the top and bottom of the guideway loops are modeled by the off-diagonal term r_{ij} . The voltages v_i are the induced loop voltages. The natural frequencies and mode shapes of this structure can be found by assuming single-frequency excitation (i.e., by modeling the effects of the moving suspension coil as a sinusoidal excitation) and by solving the resultant Eigenvalue problem.

For the purposes of calculating guideway coil self and mutual inductances to fill the inductance matrix, approximate models were developed for this guideway structure. Although the inductances can be calculated by finite element analysis, this method gives little insight into scaling laws. Therefore, several simple approximations were developed which were used as a practical design tool.

TABLE I
COMPARISON OF CALCULATIONS ON COIL GEOMETRIES

Measured inductance @ 10 kHz	Grover Calculation (using circular disk coil)	Finite Element Analysis (using actual guideway coil geometry)
259 nH	276 nH (see above)	280 nH

B. Approximate Inductance Matrix

Known solutions exist for the calculation of the inductance of geometries such as disk coils and filamentary loops. A realizable geometry for which tabulated results exist is the round loop with rectangular cross section, with mean radius a , axial length b , and width c [Fig. 6(a)]. The self-inductance of this loop may be calculated using techniques outlined in the work by Grover [26, p. 94], where the inductance is found to be

$$L = 0.1aPF. \quad (3)$$

For this calculation, a is in meters, L is in μH , and P is a function of the coil normalized radial thickness $c/2a$ [Fig. 6(b)]. For a coil of zero axial thickness (i.e., for $b = 0$), the factor $F = 1$. For $b \ll c$ and $c \ll a$ (coils resembling thin disks) the factor $F \approx 1$, an important limiting case. Therefore, for a thin disk coil with double the mean radius, there will be a corresponding doubling of the inductance.

The goal of this exercise is to approximate the complicated guideway loop geometry by a geometry where analytic expressions are available. Use of the calculation for the circular disk coil with rectangular cross section was applied to a single loop of the guideway. Shown in Fig. 7(a) is the actual geometry of one guideway loop coil which spans one pole pitch $p = 12.6$ cm. The procedure for finding an approximate equivalent disk coil [Fig. 7(b)] is as follows:

- calculate the circumference of the coil using the mean radius $l_{\text{total}} = 36.1$ cm;
- find the mean radius of a circular coil which has the same perimeter $a = 5.75$ cm;
- calculate the mean radial thickness of the coil $c = 0.39$ cm;
- find P as a function of $c/2a$ interpolating from [26, Table 26, p. 113], $P = 53.87$
- find F as a function of $c/2a$ and b/c using [26, Table 24, p. 108], $F = 0.9182$.

This methodology is designed to match the self inductance of the actual guideway coil with a circular coil. Results using $c/2a = 0.0337$ and $b/c = 0.6082$ (Table I) show good agreement between measurements made using an actual coil, finite element analysis on the coil, and the approximate calculation. This result shows the weak dependence of inductance on actual loop shape. The measured inductance (at 10 kHz) was done with a single loop and an impedance analyzer. The measured inductance is lower than the finite-element analysis value and measured value due to the skin effect.

In order to calculate the mutual inductance between coils, further approximations were made by modeling the circular disk coil considered previously by a thin filament near the center of the cross section of the disk. An approximate formula

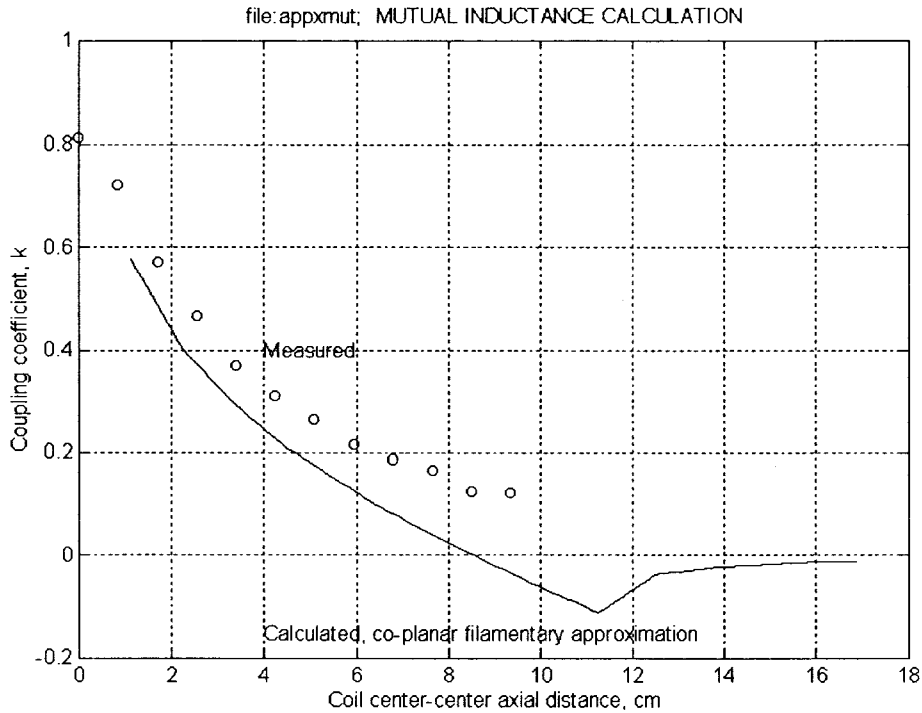


Fig. 8. Comparison of calculated (solid line) to measured guideway coil-coil mutual inductance. Mutual inductance calculation based on approximations in Butterworth.

for the calculation of the self inductance of a wire loop was first given by Maxwell [27, p. 345], where

$$L = \mu_0 a \left\{ \ln \left(\frac{8a}{r} \right) - 2 \right\} \quad (4)$$

where a is the radius of the loop in meters and r is the radius of the wire. A paper by Lyle in 1913 [28] shows that the filament approximation will give the self inductance of any circular coil with rectangular cross section to any degree of accuracy when the mean coil radius is substituted for a and the geometric mean distance (G.M.D.) is substituted for r . The values of mean radius and G.M.D. are adjusted depending on the mean radius and the cross-section profile of the coil. The same reasoning can be applied to find the mutual inductance between filamentary loops, as in the early papers by Butterworth and Campbell [29]–[31].

Using these approximation methods, the resultant self and mutual inductances were found (Fig. 8) and used to fill a 15×15 inductance matrix. The self and mutual resistances for the 15 loops was calculated and the resistance matrix was filled. This simplified calculation is compared to measurements made with actual discrete guideway coils. These matrices were used to calculate forces, dominant time constants, and the drag peak velocity with results described later in a companion paper in these TRANSACTIONS.

Once the inductance and resistance matrices are found and solved, the vectors corresponding to loop currents are used to calculate lift and drag forces. Lift force is found by

$$\langle f_z(\omega) \rangle = \frac{l}{2} \sum_{j=1}^{15} \text{Re} \{ i_j(j\omega) B_j^*(j\omega) \} \quad (5)$$

where l is a length scale associated with the horizontal length of the coil, i_j is the induced current in the j th coil, and B_j is the average field acting on the induced current. The drag force is found by evaluating the power dissipated in the guideway coils, or

$$\langle f_y(v) \rangle = \sum_{j=1}^{15} \frac{|i_j|^2}{2Rv} \quad (6)$$

where v is linear velocity and R is the loop resistance.

IV. CONCLUSIONS

The design and modeling process of a 1/5-scale “flux-canceling” maglev suspension has been described in this paper. The rotating test wheel facility has been used to measure EDS forces at various train speeds with test wheel operating speed up to 300 km/h. A set of simple techniques and models for analysis of the guideway geometry has been developed. Using approximate techniques, these models are used to predict accurately the resultant maglev lift and drag forces as a function of train speed. Test results are given in a companion paper in these TRANSACTIONS.

ACKNOWLEDGMENT

The authors gratefully acknowledge the support of the Laboratory for Electromagnetic and Electronic Systems and the Center for Transportation Studies at the Massachusetts Institute of Technology, the U.S. Department of Transportation under the Federal Railway Administration, and the Charles Stark Draper Laboratory, who provided research support.

REFERENCES

- [1] J. R. Powell and G. R. Danby, "High speed transport by magnetically suspended trains," *ASME Publ. 66 WA/RR5*, Dec. 1966.
- [2] ———, "Magnetically suspended trains for very high speed transport," in *Proc. 4th Intersociety Energy Conversion Eng. Conf.*, Washington, D.C., Sept. 22–26, 1969, pp. 953–963.
- [3] J. R. Powell and G. R. Danby, "Magnetically suspended trains: The application of superconductivity to high-speed transport," *Cryogenics Indust. Gases*, vol. 4, pp. 19–24, Oct. 1969.
- [4] C. A. Guderjahn, S. L. Wipf, H. J. Fink, R. W. Boom, K. E. MacKenzie, D. Williams, and T. Downey, "Magnetic suspension and guidance for high speed rockets by superconducting magnets," *J. Appl. Phys.*, vol. 40, no. 5, pp. 2133–2140, Apr. 1969.
- [5] C. A. Guderjahn and S. L. Wipf, "Magnetic suspension and guidance for high-speed trains by means of superconducting magnets and eddy currents," *Adv. Cryogenic Eng.*, vol. 15, pp. 117–123, June 16–18, 1969.
- [6] ———, "Magnetically levitated transportation," *Cryogenics*, pp. 171–178, June 1971.
- [7] H. H. Kolm and R. D. Thornton, "The magneplane: Guided electromagnetic flight," in *Proc. 1972 Appl. Superconductivity Conf.*, May 1–3, 1972.
- [8] D. L. Atherton, Ed., "Study of magnetic levitation and linear synchronous motor propulsion," Canadian Inst. Guided Ground Transport, Queens University, Kingston, Ontario, Annu. Rep., 1972.
- [9] R. H. Borcherts, L. C. Davis, J. R. Reitz, and D. F. Wilkie, "Baseline specifications for a magnetically suspended high-speed vehicle," *Proc. IEEE*, vol. 61, pp. 569–578, May 1973.
- [10] B. Graeminger, "Electromagnetic suspension devices," U. K. Patents 24 499, 24 541, 1912.
- [11] H. J. Fink and C. E. Hobrecht, "Instability of vehicles levitated by eddy current repulsion—Case of an infinitely long current loop," *J. Appl. Phys.*, vol. 42, no. 9, pp. 3446–3450, Aug. 1971.
- [12] L. C. Davis and D. F. Wilkie, "Analysis of motion of magnetic levitation systems: Implications for high-speed vehicles," *J. Appl. Phys.*, vol. 42, no. 12, pp. 4779–4793, Nov. 1971.
- [13] M. Iwamoto, T. Yamada, and E. Ohno, "Magnetic damping force in electro-dynamically suspended trains," *IEEE Trans. Magn.*, vol. MAG-10, pp. 458–461, 1974.
- [14] T. Yamada, M. Iwamoto, and T. Ito, "Magnetic damping force in inductive magnetic levitation system for high-speed trains," *Elec. Eng. (Japan)*, vol. 94, no. 1, pp. 80–84, 1974.
- [15] F. C. Moon, "Vibration problems in magnetic levitation and propulsion," *Transport Without Wheels*, E. Laithwaite, Ed. London, U.K.: Elek Sci., 1977, pp. 122–161.
- [16] D. Chu and F. C. Moon, "Dynamic instabilities in magnetically levitated models," *J. Appl. Phys.*, vol. 54, no. 3, pp. 1619–1625, Mar. 1983.
- [17] S. S. Chen, S. Zhu, and Y. Cai, "On unsteady-motion theory of magnetic forces for maglev systems," *J. Sound Vibration*, vol. 188, no. 4, pp. 529–543, 1995.
- [18] Y. Cai, D. M. Rote, T. M. Mulcahy, Z. Wang, S. S. Chen, and S. Zhu, "Dynamic stability of repulsive-force maglev systems," Argonne Nat. Lab., France, Rep. ANL-96/18, 1996.
- [19] R. D. Thornton, "Flux canceling maglev suspension," in *MAGLEV '93, Proc. 13th Int. Conf. Magn. Levitated Syst. Linear Drives*, Argonne Nat. Lab., Argonne, IL, May 1993.
- [20] R. D. Thornton, D. Perreault, and T. Clark, "Linear synchronous motors for maglev," U.S. Dept. Transportation, Federal Railroad Admin. Rep. DOT/FRA/NMI-92/13, Jan. 1993.
- [21] M. T. Thompson, "High temperature superconducting magnetic suspension for maglev," Ph.D. dissertation, Dep. Elec. Eng. Comput. Sci., Massachusetts Inst. Technol., Cambridge, MA, May 1997.
- [22] A. Kondoleon, D. Seltzer, R. D. Thornton, and M. T. Thompson, "Development of a large scale high speed wheel test facility," in *Proc. 3rd Int. Symp. Magn. Suspension Technol.*, Tallahassee, FL, NASA Conf. Publ. 3336, pt. 2, pp. 523–534, Dec. 13–15, 1995.
- [23] M. T. Thompson and R. D. Thornton, "Modeling of HTSC based iron-core flux-canceling electrodynamic suspension for maglev," in *Proc. 4th Int. Sym. Magn. Suspension Technol.*, Gifu, Jpn, NASA Conf. Publ., 1997.
- [24] R. D. Thornton and M. T. Thompson, "Magnetically based ride quality control for an electrodynamic maglev suspension," in *Proc. 4th Int. Symp. Magn. Suspension Technol.*, Gifu, Jpn, NASA Conf. Publ., 1997.
- [25] M. Zahn, *Electromagnetic Field Theory: A Problem Solving Approach* Malabar, FL: Krieger, 1987.
- [26] F. W. Grover, *Inductance Calculations: Working Formulas and Tables*. New York: Dover, 1946.
- [27] J. C. Maxwell, *A Treatise on Electricity and Magnetism*, vols. 1 and 2. New York: Dover, 1954.
- [28] T. R. Lyle, "On the self-inductance of circular coils of rectangular section," *Philos. Trans.*, vol. 213A, pp. 421–435, 1913.
- [29] S. Butterworth, "On the coefficients of self and mutual induction of coaxial coils," *Philos. Mag.*, vol. 29, pp. 578–592, 1915.
- [30] ———, "On the coefficients of mutual induction of eccentric coils," *Philos. Mag.*, vol. 31, pp. 443–454, 1916.
- [31] A. Campbell, "On the use of variable mutual inductances," *Philos. Mag.*, vol. 15, pp. 155–171, 1908.

Marc T. Thompson (M'92) received the B.S.E.E. degree from the Massachusetts Institute of Technology (MIT), Cambridge, MA, in 1985, the M.S.E.E. degree in 1992, the Electrical Engineer's degree in 1994, and the Ph.D. degree in 1997.

Presently, he is an engineering consultant and Adjunct Associate Professor of Electrical Engineering at Worcester Polytechnic Institute, Worcester, MA. At Worcester Polytechnic Institute, he teaches intuitive methods for analog circuit, magnetic, thermal, and power electronics design. His main research at MIT concerned the design and test of high-temperature superconducting suspensions for maglev and the implementation of magnetically based ride quality control. Other areas of his research and consulting interest include planar magnetics, power electronics, high speed analog design, induction heating, IC packaging for improved thermal and electrical performance, use of scaling laws for electrical and magnetic design, and high speed laser diode modulation techniques. He has worked as a consultant in analog, electromechanics, mechanical, and magnetics design. He also holds two patents. Currently he works on a variety of consulting projects including high power and high speed laser diode modulation, eddy-current brake design for amusement applications, flywheel energy storage for satellites, and magnetic tracking for inter-body catheter positioning. He is a consultant for Magnemotion, Inc. and Polaroid Corporation.

Richard D. Thornton (S'51–A'52–M'57–SM'75–LF'94) was formerly Professor of Electrical Engineering and Computer Science at the Massachusetts Institute of Technology (MIT), Cambridge, MA, with primary research in magnetic levitation and propulsion and power electronic control systems. In addition, he teaches and is involved in research on modeling and simulation of electronic circuits and microprocessor controlled electromagnetic and electro-mechanical systems. Starting in 1965, he worked on various transportation projects in conjunction with the DOT supported MIT Project Transport. From 1970 to 1975, he worked with Dr. Henry Kolm and others at MIT on the development of the NSF supported MIT Magneplane. He is author or co-author of three international patents on the Magneplane System. He was a member of the maglev Technical Advisory Committee, reporting to the U.S. Senate. Since 1987, the main focus of his work has been on maglev suspension, linear motor propulsion, and fault tolerant control. He has written several papers and presented many talks on the design of suspension systems and multimegawatt power electronic control systems. He has worked with members of the electric utility industry to study the proper design of electric power distribution systems for high speed ground transportation, and has also reviewed the research of others in this field. He is President of Magnemotion, Inc., Sudbury, MA.

Anthony S. Kondoleon received the B.S. degree in mechanical engineering from Northeastern University, Boston, MA, in 1972 and the M.S. degree in mechanical engineering from the Massachusetts Institute of Technology, Cambridge, MA, in 1976.

He is currently a Principle Member of the Technical Staff in the Mechanical Design and Analysis Division at Charles Stark Draper Laboratory, Cambridge, MA, and is the focal point for electro-magnetic bearing projects in the department. He has experience in the design and manufacture of inertial instruments, both mechanical and solid state. He had over five years of experience in the design, assembly, and computer analysis of precision ball bearing assemblies. He has been the principle leader in adapting automated processing to the production of precision piece part assemblies. He has authored over two dozen papers and articles on this subject over the last 20 years and holds one U.S. patent.

Mr. Kondoleon is a member of ASME.